$Ca_V1.3$ L-Type Calcium Channels Increase the Vulnerability of Substantia Nigra Dopaminergic Neurons in MPTP Mouse Model of Parkinson's Disease

Aditi Verma[1] and Vijayalakshmi Ravindranath[1,2]*

[1]*Centre for Neuroscience, Division of Biological Sciences, Indian Institute of Science, Bangalore, India, [2]Centre for Brain Research, Indian Institute of Science, Bangalore, India*

Mechanisms underlying the selective vulnerability of dopaminergic (DA) neurons in the substantia nigra pars compacta (SNpc) over those in the ventral tegmental area (VTA) to degeneration in Parkinson's disease (PD) remain poorly understood. DA neurons of SNpc and VTA are autonomous pacemakers but pacemaking in SNpc but not in VTA is accompanied by calcium influx through L-type calcium channel, $Ca_V1.3$ contributing to increased intracellular calcium and hence to cell death. $Ca_V1.3_{42A}$, an alternatively spliced short variant of $Ca_V1.3$ has increased calcium influx. We, therefore studied the role of $Ca_V1.3_{42}$ (full-length channel) and $Ca_V1.3_{42A}$ in mouse SNpc in PD pathogenesis by quantifying mRNA levels of $Ca_V1.3_{42}$ and $Ca_V1.3_{42A}$ in SNpc and followed the change in their levels in MPTP induced parkinsonism mouse model. Using *in situ* hybridization and immunohistochemistry we observed the localization of mRNA of $Ca_V1.3_{42}$ and $Ca_V1.3_{42A}$ in tyrosine hydroxylase (TH) positive DA neurons. Further, mRNA levels of $Ca_V1.3_{42A}$ were higher in SNpc as compared to the cortex. Upon MPTP treatment, mRNA levels of $Ca_V1.3_{42}$ and $Ca_V1.3_{42A}$ maintained their levels in SNpc in spite of the loss of ∼50% of the DA neurons. This indicates that the expression of $Ca_V1.3_{42}$ and $Ca_V1.3_{42A}$ is maintained at a robust level during the degenerative process in the parkinsonism model.

Keywords: neurodegeneration, SNpc, MPTP, $Ca_V1.3_{42A}$, gene expression, alternative splicing

INTRODUCTION

Parkinson's Disease (PD) is a debilitating movement disorder characterized by locomotor deficits including resting tremor, bradykinesia, rigidity and postural instability. Motor deficits result from the loss of dopaminergic (DA) neurons in the large midbrain nucleus, substantia nigra pars compacta (SNpc). SNpc DA neurons degenerate while neighboring DA neurons from the ventral tegmental area (VTA) remain relatively protected from neurodegeneration (Hirsch et al., 1988; Gibb and Lees, 1991; Dauer and Przedborski, 2003; Brichta and Greengard, 2014). A number of mechanisms have been implicated in PD neurodegeneration, namely oxidative stress possibly in relation with iron deposition (Sofic et al., 1988; Ayton and Lei, 2014), abnormal dopamine metabolism (Michel and Hefti, 1990; Pifl et al., 2014), mitochondrial dysfunction (Schapira et al., 1990; Park et al., 2009; Michel et al., 2016) and disruption of proteasomal or autophagic catabolism

(Sherman and Goldberg, 2001; Betarbet et al., 2005; Carvalho et al., 2013; Michel et al., 2016). However, in PD none of these mechanisms provides in itself an explanation for the greater vulnerability of SNpc dopaminergic neurons over DA neurons in VTA.

There is also evidence to suggest that dysregulation in calcium homeostasis could potentially account for this selectivity (Surmeier et al., 2010, 2011, 2017; Schapira, 2013; Surmeier and Schumacker, 2013). In fact, it has been reported that DA neurons from VTA express higher levels of the calcium buffering protein, calbindin-D28K (Damier et al., 1999). Besides, DA neurons in SNpc but not in VTA are characterized by pacemaking activity that is accompanied with activity of a subset of L-type voltage-dependent calcium channels having a Ca$_V$1.3 pore that elevates intracellular Ca^{2+} (Nedergaard and Greenfield, 1992; Kang and Kitai, 1993; Mercuri et al., 1994; Chan et al., 2007; Surmeier et al., 2017). However, pacemaking in VTA DA neurons appears to depend primarily on HCN/voltage-gated sodium channels (Khaliq and Bean, 2010) and the cytosolic Ca^{2+} in VTA DA neurons during pacemaking is reported to be significantly less as compared to that in DA neurons in SNpc (Guzman et al., 2018). This has led to the hypothesis that Ca^{2+}-dependent pacemaking along with a poor calcium buffering capacity may cause calcium overload through L-type Ca$_V$1.3 channel activation in most vulnerable DA SNpc neurons making them preferentially at risk to degeneration (Surmeier et al., 2010, 2017; Liss and Striessnig, 2019).

Several alternatively spliced variants of the full-length channel Ca$_V$1.3$_{42}$ have been reported, among them is Ca$_V$1.3$_{42A}$, a short splice variant that incorporates in a mutually exclusive manner, exon 42A instead of exon 42 (Bock et al., 2011; Huang et al., 2013). Exon 42A contains a stop codon and translation of the protein terminates before encoding the C-terminal modulatory domain, which results in a splice variant product with different electrophysiological properties compared to the full-length channel. The calcium current density through Ca$_V$1.3$_{42A}$ is about 2.5 times greater than in Ca$_V$1.3$_{42}$ (Singh et al., 2008). Further, it has been reported that the activation range of Ca$_V$1.3$_{42A}$ is shifted to a more negative potential by ~10 mV (Singh et al., 2008). Moreover, these variants show greater insensitivity to inhibition by dihydropyridines (DHPs) as compared to other C-terminus variants and the full-length channel (Huang et al., 2013). Thus, the activation potential of Ca$_V$1.3$_{42A}$ is closer to the resting membrane potential and there is greater calcium influx through this variant as compared to other C-terminus variants and full-length channel (Tan et al., 2011; Huang et al., 2013). Further, the presence of these channels has been demonstrated in the mouse and human brain (Singh et al., 2008; Bock et al., 2011).

Owing to the atypical electrophysiological properties of Ca$_V$1.3$_{42A}$, we hypothesized that the expression of this splice variant in SNpc could potentially play a role in DA cell death by causing perturbations in calcium homeostasis. To this aim we studied the expression of mRNA encoding Ca$_V$1.3$_{42A}$ and Ca$_V$1.3$_{42}$ (full-length) in midbrain DA neurons in naïve mice and evaluated if the transcription of these channels was affected during neurodegeneration mediated by MPTP in mouse model of PD.

MATERIALS AND METHODS

Animals and MPTP Dosing

Animal experiments were carried out on C57BL/6J male mice (3–4 months; 25–30 g) procured from Central Animal Facility of Indian Institute of Science, Bangalore, India. All animal experiments were carried out according to institutional guidelines for the use and care of animals. Animal experiments were approved by the institutional animal ethical review board, named "Institutional Animal and Ethics Committee" of the Indian Institute of Science (Protocol# CAF/Ethics/267/2012). Handling of animals was done according to the guidelines of the Committee for the Purpose of Control and Supervision of Experiments on Animals (CPCSEA), Government of India. All experiments were performed in adherence to ARRIVE guidelines. All efforts were made to minimize animal suffering, reduce the number of animals used and to use alternatives to *in vivo* techniques, if available. Animals were housed in groups and had access to pelleted diet and water, *ad libitum*. The sample size for experiments with untreated animals was 6–11. For the MPTP mouse model of dopaminergic loss (Jackson-Lewis and Przedborski, 2007), 30 mg/kg body weight 1-methyl-4-phenyl-1,2,3,6-tetrahydropyridine (MPTP; Sigma–Aldrich Cat# M0896) dissolved in normal saline was given subcutaneously to the mice as a single dose or daily for 14 days. MPTP injections were carried out in an isolated clean air room in the Central Animal Facility, Indian Institute of Science, Bangalore, India. The controls were injected with an equivalent volume of normal saline. Animals were allocated to treated or control groups in a random manner. The sample sizes for MPTP experiments were 4–11 for each group. Animals were sacrificed 24 h after the last MPTP dose.

Adequate safety precautions were followed in the proper handling of MPTP during preparation and injection, and in the disposal of materials and samples contaminated with MPTP and its metabolites. Protective gear was worn during the preparation and injection of MPTP. Syringes and needles that were used for injection were incinerated after a single-use. Mice undergoing MPTP treatment were housed in separate cages and the contaminated bedding material and feed were incinerated upon disposal.

Mouse Brain Dissection

Animals were decapitated following cervical dislocation. Cortex, ventral midbrain and striatum were dissected out under cold and sterile conditions. For dissection of SNpc, the whole mouse brain was placed on mouse brain matrix (Ted Pella, Inc., Cat# 15050) and 1 mm thick slices of the brain were obtained. Then, SNpc was dissected out from these slices under a dissecting stereomicroscope using anatomical markers.

RNA Isolation and cDNA Synthesis

All the reagents and glassware used for RNA isolation, cDNA synthesis, *in situ* hybridization and immunohistochemistry

were made RNAse free. RNA from mouse brain tissue was isolated using TRIzol reagent (Invitrogen Cat# 15596018) and bromochlorophenol (BCP; Moelcular Research Centre, Inc., Cat# BP151; Chomczynski and Sacchi, 2006). Total RNA (500 ng) was used for first-strand cDNA synthesis using random hexamers, dNTPs and reverse transcriptase from the High capacity cDNA reverse transcription kit (Applied Biosystems Cat# 4368814).

Quantitative Real-Time PCR

Quantitative real-time PCR (qRT-PCR) was performed using SYBR green chemistry with primer pairs designed to distinguish the full-length Ca$_V$1.3 and splice variant. The nucleotide sequences for primers used for mouse gene expression analysis and the PCR conditions are provided in **Supplementary Tables S1, S2**, respectively. Further, the specificity of the primers as assessed by the presence of a single band at the desired size measured through gel electrophoresis has been represented in **Supplementary Figure S1**. Three endogenous controls, namely 18S rRNA, β-actin and GAPDH were used for normalization when cDNA from untreated mouse tissue was analyzed. β-actin and/or GAPDH normalization was performed in subsequent experiments as reported. Further, cell-type-specific normalizations were performed with tyrosine hydroxylase (TH), DAT, GAD1, and VGlut2. The samples were analyzed in duplicates or triplicates. Data from all samples have been reported and no exclusion of outliers has been performed.

Fluorescent *in situ* Hybridization (FISH) and Immunohistochemistry

Male C57BL/6J mice brains were isolated and fixed in 4% paraformaldehyde (w/v) for 12 h following decapitation after cervical dislocation. Fixed brains were then allowed to sink in 30% sucrose before embedding in tissue freezing system (Leica Microsystems Nussloch GmbH Cat# 0201 08926). Coronal sections measuring 14 μm in thickness were cut through midbrain under RNAse free conditions using a Cryostat (Leica Microsystems). The sections were hydrated, acetylated and treated with 25 μg of proteinase K (Roche Cat# 03115852001) for 7 min at 37°C. The sections were then rinsed with phosphate buffer and dehydrated using ethanol gradient. Digoxigenin-labeled sense (control) and antisense RNA probes were synthesized using SP6 and T7 polymerases (Roche Cat# 11175025910), respectively from Ca$_V$1.3$_{42}$ and Ca$_V$1.3$_{42A}$ cDNA sequences that were cloned into dual promoter pCRII vector (Invitrogen Cat# K206001). The sequences of the primers used for Ca$_V$1.3$_{42}$ and Ca$_V$1.3$_{42A}$ amplification are as follows: mouse Ca$_V$1.3$_{42}$, full-length (NM_028981.2; Forward, GGGAAAGTACCCTGCGAAGAACACC; Reverse, GGATTTCTGGCCCAATGTCATGCAG) and Ca$_V$1.3$_{42A}$, splice variant (Forward, CAGATGCTTGAACGGATGCTTTAG; Reverse, CTTCCTTCCGGAGGAGTGC). The sections were hybridized with sense and antisense probes (100 ng/μl) overnight in a humid chamber at 45°C followed by washing, incubation with 0.5% blocking agent (from Invitrogen TSA Kit #21 Cat# T20931). Signal was developed using a peroxidase-labeled anti-DIG antibody (Roche Cat# 11207733910) at a concentration of 1 in 250 followed by tyramide signal

amplification (Invitrogen TSA Kit #21 Cat# T20931) and finally incubation with fluorescein-conjugated streptavidin (Vector Laboratories Cat# SA-5001) at a concentration of 1 in 500. Absence of fluorescence signal on the sections hybridized with the sense probes has been represented in **Supplementary Figure S2**.

Immunohistochemistry (IHC) was performed for investigating the co-localization of the expression of calcium channel isoforms with marker of DA neurons, TH. IHC was performed on the same sections on which FISH was performed. The sections were first rinsed in phosphate buffer followed by blocking and overnight incubation in anti-TH rabbit antibody (Millipore Cat# AB152, RRID:AB_390204). Sections were then washed and incubated in Goat Anti-Rabbit IgG H+L (Alexa Fluor® 594; Thermo Fisher Scientific, Cat# A-21207, RRID:AB_141637) followed by washing. The sections were then mounted in Vectashield® mounting medium (Vector Laboratories Cat# H-1000) and imaged as z-stacks using a Zeiss LSM 780 confocal microscope using LD LCI plan-apochromat 25×/0.8 Oil objective using 488 nm and 594 nm lasers for low magnification images and plan-apochromat 100×/1.4 Oil objective using 488 nm and 594 nm lasers for high magnification images. The maximum intensity projection that is used for representation was derived using Zeiss ZEN black software and orthogonal reconstruction was performed using Zeiss ZEN blue software.

Statistical Analyses

Analysis of relative gene expression from the qRT-PCR data was done using ΔΔCt method. The thresholds were set manually. Data were analyzed using Graphpad Prism (Graphpad Prism Inc., San Diego, CA, USA). Shapiro–Wilk test was performed on all datasets to test for normality and statistical tests were carried out accordingly. Statistical significance was determined using one-way ANOVA followed by student's Newman–Keuls post-test for multiple comparisons and student's *t*-test for comparison between two groups for data that passed normality test. Two-tailed Mann–Whitney-U test was used for comparison between two groups when the data did not pass the test for normality.

RESULTS

Ca$_V$1.3$_{42A}$ and Ca$_V$1.3$_{42}$ Expression in Ventral Midbrain, Cortex, and Striatum in Mice

mRNA levels of Ca$_V$1.3$_{42A}$ and Ca$_V$1.3$_{42}$ were assayed in the ventral midbrain of C57BL/6J naïve mice using qRT-PCR. mRNA levels for Ca$_V$1.3$_{42A}$, the short splice variant of Ca$_V$1.3 containing exon 42A, were four times greater in the ventral midbrain as compared to the cortex and striatum (**Figure 1A**). Conversely, mRNA levels of full-length Ca$_V$1.3 (Ca$_V$1.3$_{42}$) were greater in the cortex and striatum than in the ventral midbrain (**Figure 1B**). When comparing relative mRNA levels for Ca$_V$1.3$_{42A}$ and Ca$_V$1.3$_{42}$, we found that Ca$_V$1.3$_{42A}$
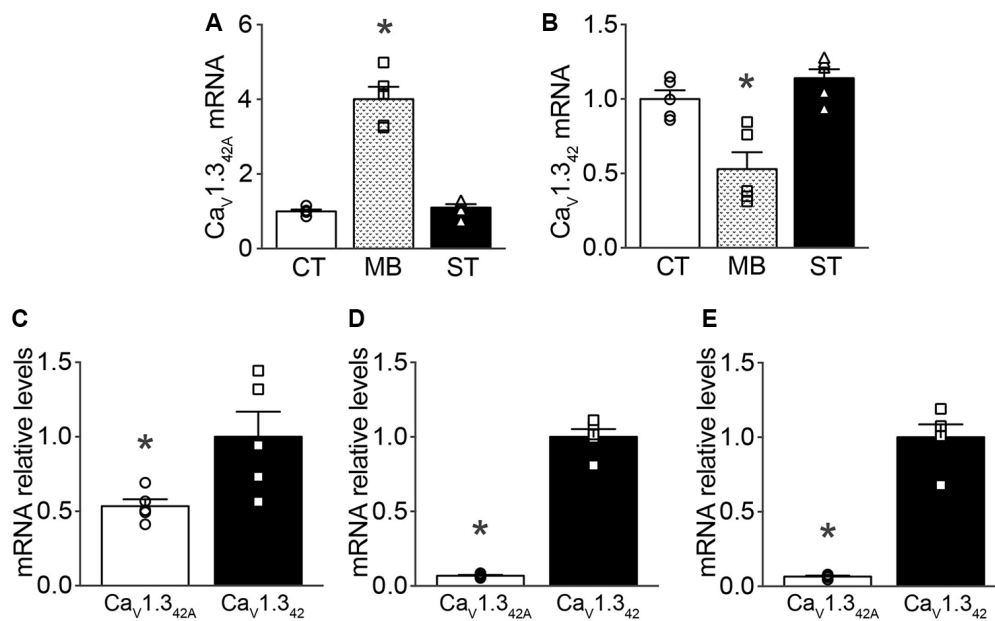
FIGURE 1 | $Ca_V1.3_{42}$ and $Ca_V1.3_{42A}$ mRNA expression levels in mouse brain regions as measured by qRT-PCR. **(A)** Expression of $Ca_V1.3_{42A}$ ($F_{(2,12)} = 15.54$, $p = 0.0005$), **(B)** $Ca_V1.3_{42}$ ($F_{(2,12)} = 73.22$, $p < 0.0001$) in the ventral midbrain (MB) in comparison to expression profiles in the cortex (CT) and striatum (ST). Panels **(C–E)** describe the relative expression of $Ca_V1.3_{42A}$ to $Ca_V1.3_{42}$ in ventral midbrain ($p = 0.0281$, $t = 2.675$, $df = 8$), cortex ($p < 0.0001$, $t = 17.78$, $df = 8$) and striatum ($p < 0.0001$, $t = 10.86$, $df = 8$), respectively. Data were normalized to mean of 18S rRNA, β-actin and GAPDH as endogenous controls. Each dot in the figure represents an individual animal. One-way ANOVA with Newman–Keuls test was performed for multiple comparisons and unpaired, two-tailed student's t-test was performed for pair-wise comparisons on the data. Data represented as mean ± SEM. *$p < 0.05$.

mRNA levels represented about 0.5 times that of $Ca_V1.3_{42}$ in the ventral midbrain (**Figure 1C**). However, in the cortex and striatum mRNAs encoding $Ca_V1.3_{42A}$ were much less abundant (approximately 0.06 times) than mRNAs for $Ca_V1.3_{42}$ (**Figures 1D,E**, respectively).

Co-localization of $Ca_V1.3_{42A}$ and $Ca_V1.3_{42}$ With TH Positive Dopaminergic Neurons in SNpc
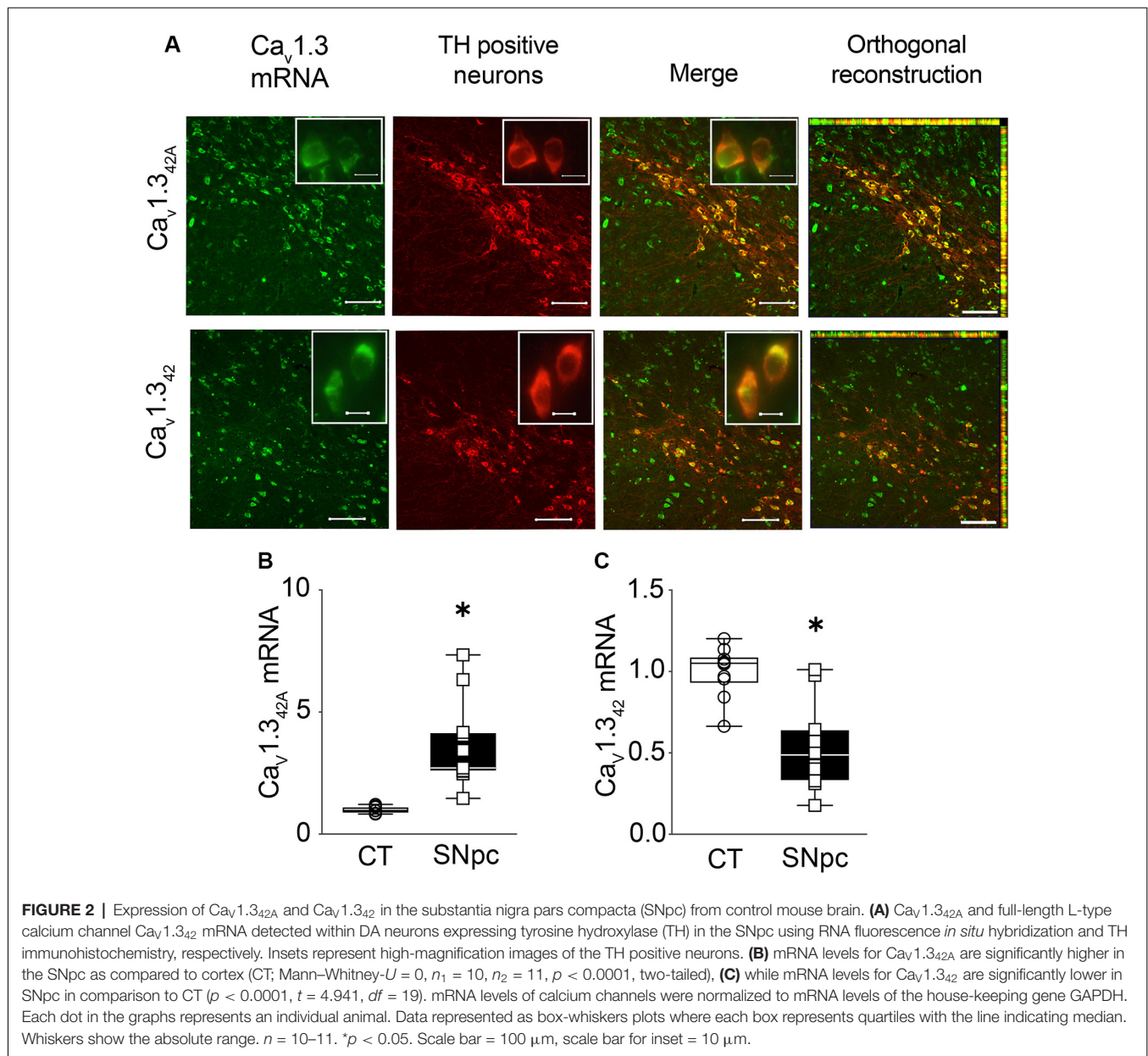
The available antibodies against $Ca_V1.3$ are highly non-specific. Therefore, *in situ* hybridization was used to identify and localize the expression of $Ca_V1.3_{42A}$ and $Ca_V1.3_{42}$ in the midbrain. Combined fluorescent *in situ* hybridization for $Ca_V1.3_{42A}$ and immunohistochemistry for TH allowed us to demonstrate that mRNAs encoding the short splice variant were present in SNpc DA neurons in control mice as indicated by orthogonal reconstruction (**Figure 2A**). Likewise, $Ca_V1.3_{42}$ mRNA was also co-localized with TH positive neurons in SNpc as seen from orthogonal reconstruction (**Figure 2A**). When using qRT-PCR, we found that mRNA levels of $Ca_V1.3_{42A}$ were approximately four-fold higher in the SNpc as compared to the cortex (**Figure 2B**). In contrast, mRNA levels for the full-length channel $Ca_V1.3_{42}$ were lower in the SNpc as compared to the cortex (**Figure 2C**). These observations are also consistent with mRNA expression data reported for $Ca_V1.3_{42}$ and $Ca_V1.3_{42A}$ in the midbrain and cortex in **Figure 1**.

mRNA Levels of $Ca_V1.3_{42A}$ and $Ca_V1.3_{42}$ in SNpc After Acute Exposure to MPTP

MPTP, which is known to cause a selective loss of DA neurons in SNpc when administered to mice serves as a model of neurodegeneration akin to that seen in PD. In the present study, male C57BL/J6 mice received a single dose of MPTP (30 mg/kg body weight dose) administered subcutaneously. The animals were sacrificed 1 day after the dose. A single dose of MPTP did not result in the loss of TH mRNA levels in the SNpc (**Figure 3A**).

Subsequently, mRNA levels of $Ca_V1.3_{42A}$ and $Ca_V1.3_{42}$ were assessed in SNpc. However, normalization of $Ca_V1.3_{42A}$ and $Ca_V1.3_{42}$ mRNA to TH mRNA revealed that the expression of mRNA encoding $Ca_V1.3_{42A}$ was significantly increased in the SNpc (**Figure 3B**) while $Ca_V1.3_{42}$ presented no significant change in mRNA expression (**Figure 3C**).

These results were further validated by using dopamine transporter (DAT) as another marker for dopaminergic neurons. MPTP treatment did not result in significant loss of DAT mRNA transcript levels in SNpc (**Figure 3D**). Upon normalization of $Ca_V1.3_{42A}$ and $Ca_V1.3_{42}$ to DAT mRNA, there was a statistically significant increase in mRNA expression of $Ca_V1.3_{42A}$ (**Figure 3E**) but there was no significant difference in expression of $Ca_V1.3_{42}$ mRNA (**Figure 3F**). There was also no significant change when $Ca_V1.3_{42A}$ and $Ca_V1.3_{42}$ mRNA levels were normalized to mRNA levels for glutamate decarboxylase 1 (GAD1) and vesicular glutamate transporter 2 (Vglut2), markers of GABAergic (**Figures 3G,H**) and glutamatergic (**Figures 3I,J**)

FIGURE 2 | Expression of $Ca_V1.3_{42A}$ and $Ca_V1.3_{42}$ in the substantia nigra pars compacta (SNpc) from control mouse brain. **(A)** $Ca_V1.3_{42A}$ and full-length L-type calcium channel $Ca_V1.3_{42}$ mRNA detected within DA neurons expressing tyrosine hydroxylase (TH) in the SNpc using RNA fluorescence *in situ* hybridization and TH immunohistochemistry, respectively. Insets represent high-magnification images of the TH positive neurons. **(B)** mRNA levels for $Ca_V1.3_{42A}$ are significantly higher in the SNpc as compared to cortex (CT; Mann–Whitney-$U = 0$, $n_1 = 10$, $n_2 = 11$, $p < 0.0001$, two-tailed), **(C)** while mRNA levels for $Ca_V1.3_{42}$ are significantly lower in SNpc in comparison to CT ($p < 0.0001$, $t = 4.941$, $df = 19$). mRNA levels of calcium channels were normalized to mRNA levels of the house-keeping gene GAPDH. Each dot in the graphs represents an individual animal. Data represented as box-whiskers plots where each box represents quartiles with the line indicating median. Whiskers show the absolute range. $n = 10$–11. *$p < 0.05$. Scale bar = 100 μm, scale bar for inset = 10 μm.

neurons, respectively. Our results indicate the differential expression of $Ca_V1.3_{42A}$ but not of $Ca_V1.3_{42}$ following acute exposure to MPTP.

mRNA Levels of $Ca_V1.3_{42A}$ and $Ca_V1.3_{42}$ in SNpc After Sub-chronic Exposure to MPTP

Further, to assess the effect of sub-chronic exposure to MPTP on the mRNA expression of $Ca_V1.3_{42A}$ and $Ca_V1.3_{42}$, male C57BL/J6 mice received MPTP that was administered subcutaneously once a day for 14 days. This treatment regimen resulted in a 45% loss of TH mRNA levels in the SNpc (**Figure 4A**).

mRNA levels of $Ca_V1.3_{42A}$ and $Ca_V1.3_{42}$ were then assessed in SNpc. Normalization of $Ca_V1.3_{42A}$ and $Ca_V1.3_{42}$ mRNA to TH mRNA resulted in significantly increased expression

of mRNA encoding $Ca_V1.3_{42A}$ and $Ca_V1.3_{42}$, respectively, in the SNpc (**Figures 4B,C**). Further, MPTP treatment resulted in a 47% loss of DAT mRNA transcript levels in SNpc (**Figure 4D**). Upon normalization of $Ca_V1.3_{42A}$ and $Ca_V1.3_{42}$ to DAT mRNA, there was a statistically significant increase in mRNA expression (**Figures 4E,F**). Moreover, the increased expression of $Ca_V1.3_{42A}$ or $Ca_V1.3_{42}$ mRNA was not observed in the VTA from animals after sub-chronic MPTP exposure (**Supplementary Figure S3**). MPTP treatment did not change the expression of GAD1 (**Figure 4G**) and VGlut2 (**Figure 4J**). No significant difference in mRNA expression was observed when $Ca_V1.3_{42A}$ and $Ca_V1.3_{42}$ mRNA levels were normalized to mRNA levels for GAD1 (**Figures 4H,I**) and Vglut2 (**Figures 4K,L**) and β-actin (**Figures 4M,N**), respectively.
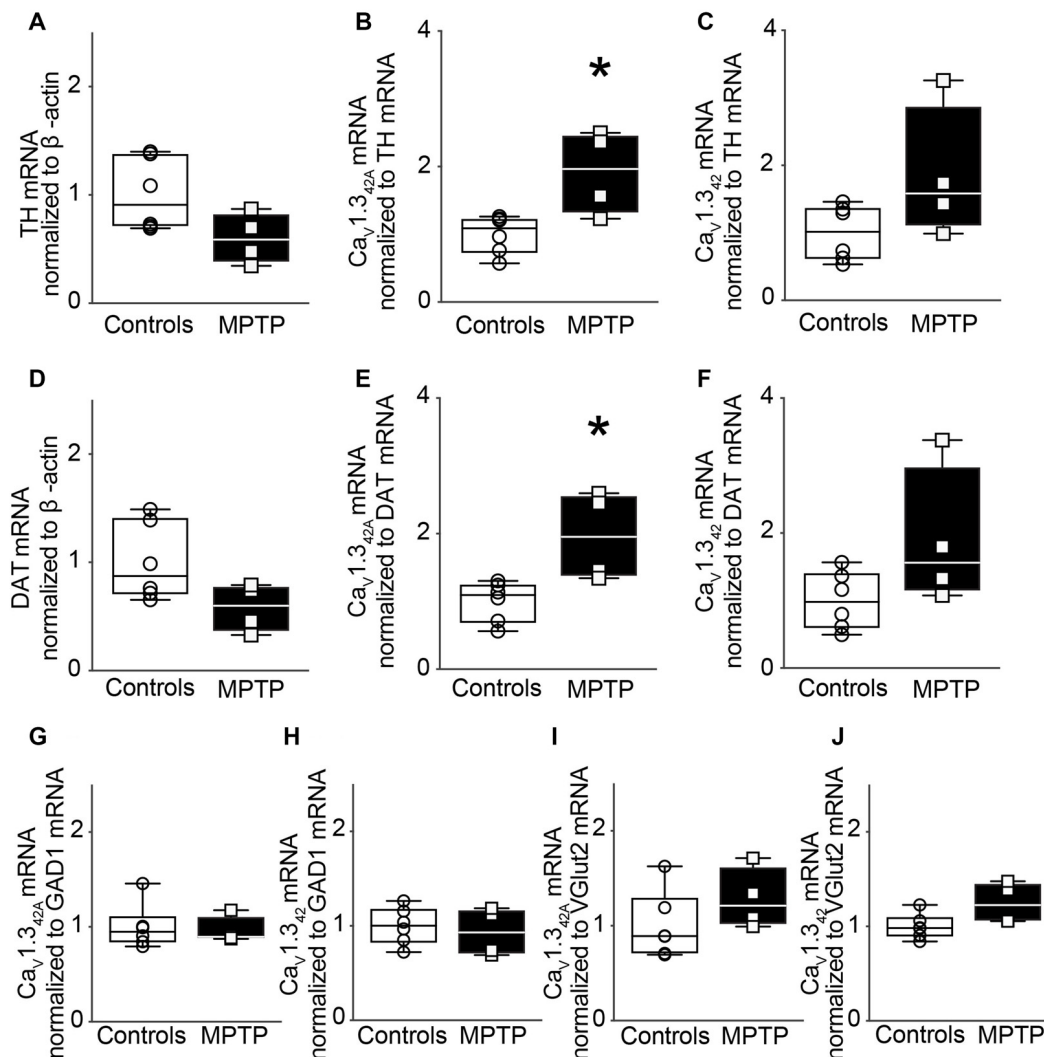
FIGURE 3 | Modulation of Ca$_V$1.3$_{42A}$ but not Ca$_V$1.3$_{42}$ mRNA levels in the SNpc of MPTP-treated mice after 1 day of treatment. **(A)** TH mRNA expression in the SNpc of mice treated subcutaneously with a single dose of MPTP (30 mg/kg body weight) and sacrificed after 1 day. MPTP treatment did not lead to a change in TH mRNA levels in the SNpc ($p = 0.0722$, $t = 2.070$, $df = 8$). qRT-PCR data were normalized to mRNA levels of β-actin. **(B)** Relative mRNA levels for Ca$_V$1.3$_{42A}$ ($p = 0.0121$, $t = 3.229$, $df = 8$) increased in the SNpc in response to MPTP treatment and **(C)** Ca$_V$1.3$_{42}$ ($p = 0.0901$, $t = 1.927$, $df = 8$) did not change significantly when the mRNA signal was normalized to TH. **(D)** mRNA levels of DAT did not change upon MPTP treatment when normalized to mRNA levels of β-actin ($p = 0.0733$, $t = 2.061$, $df = 8$). **(E)** Relative mRNA levels for Ca$_V$1.3$_{42A}$ ($p = 0.0126$, $t = 3.198$, $df = 8$) increased in the SNpc in response to MPTP treatment while **(F)** Ca$_V$1.3$_{42}$ ($p = 0.899$, $t = 1.929$, $df = 8$) were not significantly different when the mRNA signal was normalized to DAT mRNA levels. **(G)** mRNA levels for Ca$_V$1.3$_{42A}$ (Mann–Whitney-$U = 11$, $n_1 = 6$, $n_2 = 4$, $p = 0.9143$, two-tailed) and **(H)** Ca$_V$1.3$_{42}$ ($p = 0.6589$, $t = 0.4584$, $df = 8$) were found to be unchanged in the SNpc of MPTP-treated mice upon normalization to GAD1. **(I)** mRNA levels for Ca$_V$1.3$_{42A}$ ($p = 0.2405$, $t = 1.268$, $df = 8$) and **(J)** Ca$_V$1.3$_{42}$ ($p = 0.0562$, $t = 2.232$, $df = 8$) were also found to be unchanged in the SNpc of MPTP-treated mice upon normalization to Vglut2. Each point represents an individual animal. For controls $n = 6$, for MPTP treated samples, $n = 4$. Unpaired, two-tailed student's t-test or two-tailed Mann–Whitney-U test has been performed on each control vs. MPTP comparison. Data represented as box-whiskers plots where each box represents quartiles with the line indicating median. Whiskers show the absolute range. *$p < 0.05$.

DISCUSSION

It has been postulated that Ca$_V$1.3 L-type calcium channels, which contribute to the pacemaking activity of SNpc DA neurons may also play a role in their vulnerability to degeneration. Indeed, autonomous pacemaking leads to increase in basal mitochondrial oxidative stress in SNpc DA neurons, presumably as a direct consequence of the Ca^{2+} load (Foehring et al., 2009; Guzman et al., 2010; Surmeier et al., 2017; Liss and Striessnig, 2019). In support of this hypothesis, it has been shown that blocking Ca$_V$1.3 with a calcium channel antagonist, isradipine, afforded protection against neurodegeneration in the MPTP, 6-OHDA and rotenone rodent model of PD (Chan et al., 2007, 2010; Ilijic et al., 2011). Further, Guzman et. al. have demonstrated that chronic, systemic isradipine treatment led to reduced cytosolic Ca^{2+} in SNpc
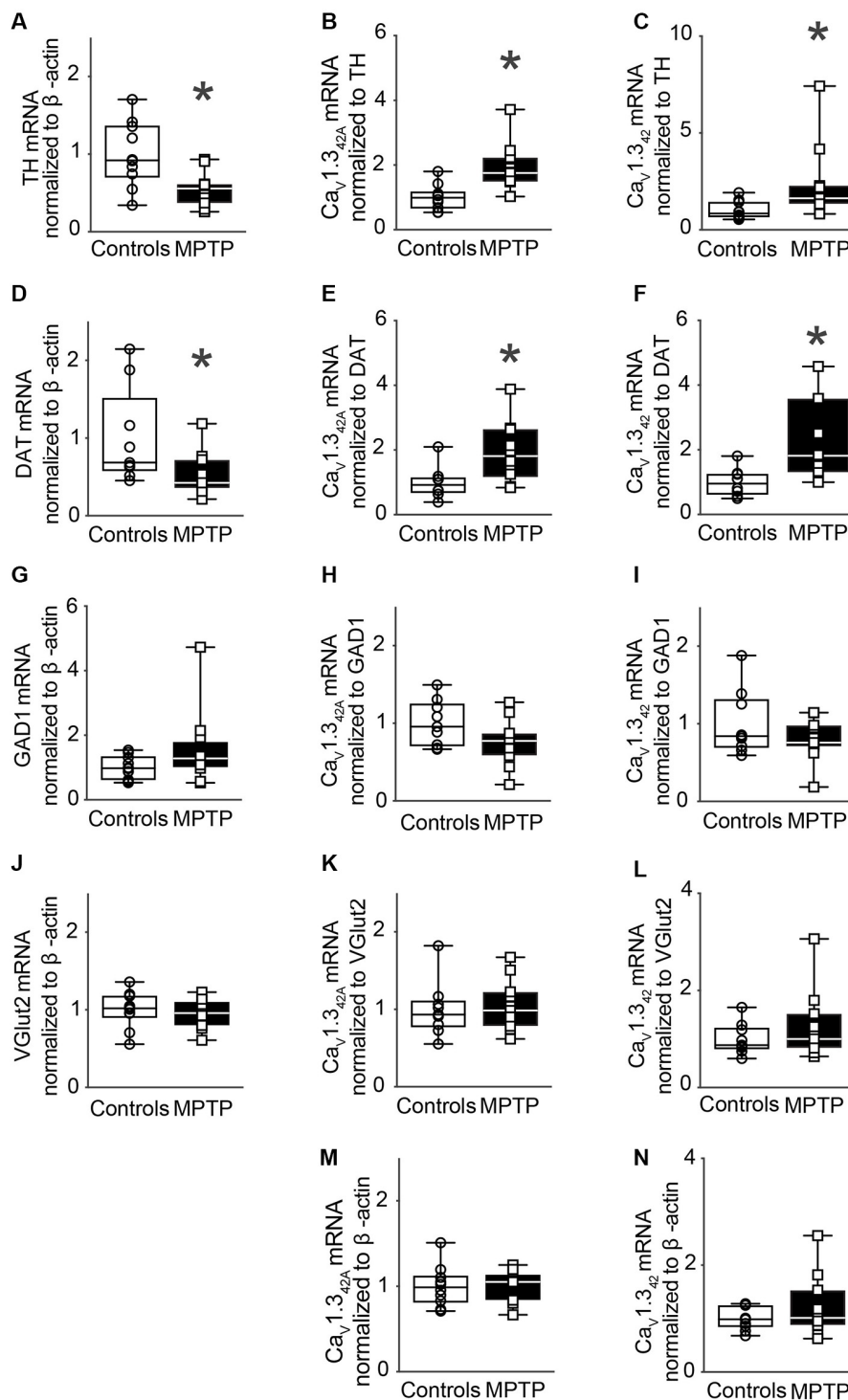
FIGURE 4 | Modulation of Ca$_V$1.3$_{42A}$ and Ca$_V$1.3$_{42}$ mRNA levels in the SNpc of MPTP-treated mice after 14 days of treatment. **(A)** TH mRNA expression in the SNpc of mice treated subcutaneously with MPTP (30 mg/kg body weight) for 14 days. MPTP treatment led to a 45% reduction of TH mRNA levels in the SNpc ($p = 0.0052$, $t = 3.152$, $df = 19$). qRT-PCR data were normalized to mRNA levels of β-actin. **(B)** Relative mRNA levels for Ca$_V$1.3$_{42A}$ ($p = 0.0048$, $t = 3.19$, $df = 19$) and **(C)** Ca$_V$1.3$_{42}$ (Mann–Whitney $U = 17$, $n_1 = 10$, $n_2 = 11$, $p = 0.0062$, two-tailed) increased in the SNpc in response to MPTP treatment when the mRNA signal was normalized to TH. **(D)** mRNA levels of DAT were reduced by 47% upon MPTP treatment when normalized to mRNA levels of β-actin (Mann–Whitney-$U = 19$, $n_1 = 9$, $n_2 = 11$, $p = 0.0200$, two-tailed). **(E)** Relative mRNA levels for Ca$_V$1.3$_{42A}$ ($p = 0.0227$, $t = 2.522$, $df = 16$) and **(F)** Ca$_V$1.3$_{42}$ ($p = 0.0114$, $t = 2.859$, $df = 16$)

(*Continued*)

FIGURE 4 | Continued

increased in the SNpc in response to MPTP treatment when the mRNA signal was normalized to DAT mRNA levels. **(G)** mRNA levels of GAD1 remained unchanged when normalized to β-actin (Mann–Whitney-U = 41, n_1 = 10, n_2 = 11, p = 0.2276, two-tailed). **(H)** mRNA levels for $Ca_V1.3_{42A}$ (p = 0.0787, t = 1.864, df = 18) and **(I)** $Ca_V1.3_{42}$ (p = 0.2097, t = 1.301, df = 18) were found to be unchanged in the SNpc of MPTP-treated mice upon normalization to GAD1. **(J)** mRNA levels of VGlut2 remained unchanged when normalized to β-actin (p = 0.5594, t = 0.5936, df = 20). **(K)** mRNA levels for $Ca_V1.3_{42A}$ (p = 0.7443, t = 0.3312, df = 18) and **(L)** $Ca_V1.3_{42}$ (Mann–Whitney-U = 43, n_1 = 9, n_2 = 11, p = 0.6556, two-tailed) were found to be unchanged in the SNpc of MPTP-treated mice upon normalization to Vglut2. **(M)** mRNA levels for $Ca_V1.3_{42A}$ (p = 0.8383, t = 0.2069, df = 19) and **(N)** $Ca_V1.3_{42}$ (p = 0.2777, t = 1.118, df = 19) were found to be unchanged in response to MPTP treatment upon normalization to β-actin. Each point represents an individual animal. For controls n = 9–10, for MPTP treated samples, n = 10–12. Unpaired, two-tailed student's t-test or two-tailed Mann–Whitney-U test was performed on each control vs. MPTP comparison. Data are represented as box-whiskers plots where each box represents quartiles with the line indicating median. Whiskers show the absolute range. *Indicates $p < 0.05$.

DA neurons and lowered mitochondrial oxidant stress. It has been shown that knockdown of $Ca_V1.3$ resulted in reduced dendritic Ca^{2+} oscillations in SNpc DA neurons elucidating their importance in the process (Guzman et al., 2018). This prompted us to study the expression of mRNAs encoding the full-length channel $Ca_V1.3_{42}$ and its C-terminally truncated splice variant $Ca_V1.3_{42A}$ in SNpc. Besides, we evaluated the transcripts of the two-channel isoforms in the MPTP mouse model of PD.

The qRT-PCR analysis revealed that $Ca_V1.3_{42A}$ transcripts were expressed more abundantly in the ventral midbrain including SNpc when compared to the cortex, whereas the opposite was true for $Ca_V1.3_{42}$ transcripts. Interestingly, mRNAs encoding the full-length channel $Ca_V1.3_{42}$ as well as its truncated splice variant $Ca_V1.3_{42A}$ were found to be selectively increased in the SNpc of MPTP-treated mice.

While the presence of the full-length isoform of $Ca_V1.3$ channels $Ca_V1.3_{42}$ and that of its short splice variant $Ca_V1.3_{42A}$ has been reported in the mouse (Bock et al., 2011; Tan et al., 2011) and human brain (Singh et al., 2008), there is no study comparing the regional expression of the two mRNA isoforms in the brain. By coupling *in situ* hybridization to immunohistochemistry, we demonstrated that both $Ca_V1.3_{42}$ and $Ca_V1.3_{42A}$ mRNA expressed in TH positive neurons in the SNpc. Furthermore, we showed that mRNA levels for the splice variant $Ca_V1.3_{42A}$ were higher in mouse ventral midbrain as compared to cortex or striatum whereas the opposite was true for $Ca_V1.3_{42}$ transcripts. $Ca_V1.3_{42A}$ mRNA expression was also higher in the SNpc in comparison to the cortex in concurrence with the above. This indicates that the L-type calcium channel isoform $Ca_V1.3_{42A}$ substantially contributes to calcium influx in midbrain DA neurons in the SNpc. Since calcium current density through $Ca_V1.3_{42A}$ is about 2.5 times greater than the full-length channel isoform (Singh et al., 2008), one may assume that calcium influx through this channel is more pronounced in midbrain DA neurons than cortical neurons. It may be noted that the pacemaking activity inherent to DA neurons is

accompanied by $Ca_V1.3$ L-type calcium channels in the SNpc but not in the VTA where it relies on Na_V/HCN channels (Guzman et al., 2010; Khaliq and Bean, 2010). This may render nigral DA neurons more vulnerable to calcium overload through activation of $Ca_V1.3_{42A}$ channels. The differential vulnerability between SNpc and VTA DA neurons may be further exacerbated by the fact that DA neurons from the VTA also contain high levels of the calcium buffering protein Calbindin-D28K while most vulnerable DA neurons in the SNpc are lacking this protein (Damier et al., 1999).

In the present study, we also examined mRNA expression changes, if any, of the L-type calcium channel and its variant in the SNpc in response to both acute and sub-chronic treatment regimens with the DA neurotoxin MPTP. In fact, the expression of $Ca_V1.3_{42A}$ was significantly higher in SNpc after 24 h of MPTP exposure although the levels of TH and DAT mRNA were not significantly affected (**Figure 3**). However, after 14 days of MPTP treatment, when the TH and DAT mRNA levels were reduced by approximately 50%, the mRNA levels of $Ca_V1.3_{42}$ and $Ca_V1.3_{42A}$ were maintained and were similar to vehicle controls. Since $Ca_V1.3_{42}$ and $Ca_V1.3_{42A}$ are predominantly expressed in SNpc by DA neurons, a ~50% reduction of the number of these neurons induced by sub-chronic MPTP treatment should be reflected by a significant decrease in transcripts encoding the two-channel isoforms. This was not the case, however, upon normalization to β-actin indicating that there is a compensatory increase in the expression of the channel transcripts in the surviving SNpc DA neurons. Further, when mRNA expression for $Ca_V1.3_{42}$ and $Ca_V1.3_{42A}$ was normalized to TH and DAT mRNA, we observed a significant increase in transcripts encoding $Ca_V1.3_{42A}$ after 1 day of single dose of MPTP and both channel isoforms after 14 days of exposure to MPTP. This suggested that DA neurons may produce more transcripts to possibly preserve their activity in surviving neurons in response to neurodegeneration triggers.

In rodents, while about 70% of SNpc neurons are DA neurons, about 29% of SNpc neurons are GABAergic and about 1–2% are glutamatergic (Nair-Roberts et al., 2008). It was, therefore, essential to demonstrate that the increased expression of $Ca_V1.3_{42}$ and $Ca_V1.3_{42A}$ mRNA resulted from the loss of DA neurons after MPTP treatment and not from changes affecting other neuronal populations. Consistent with this view, the expression of $Ca_V1.3_{42}$ and $Ca_V1.3_{42A}$ transcripts remained unchanged in the SNpc when mRNA signals were normalized to either mRNA for GAD1, a GABAergic neuron marker or for Vglut2, a glutamatergic neuron marker.

The upregulation observed in the expression of $Ca_V1.3_{42A}$ and $Ca_V1.3_{42}$ mRNA upon normalization to TH and DAT mRNA levels could, therefore, have the following plausible explanations: (i) While the observed change in the expression of $Ca_V1.3$ channels in MPTP treated mouse SNpc could be explained as a retention of phenotype, it is important to note that about 50% loss in the number of TH positive neurons along with loss of Nissl positive neurons has been observed in the SNpc of MPTP treated mice (Saeed et al., 2009). Since $Ca_V1.3$ channels are expressed in neurons, a resultant reduction in their mRNA expression in SNpc is, therefore, expected

concomitant to the reduction in the number of TH positive neurons in SNpc similar to that seen for the mRNA expression of TH and DAT. (ii) The $Ca_V1.3_{42A}$ and $Ca_V1.3_{42}$ mRNA upregulation could be a result of their upregulation in non-TH expressing (non-dopaminergic) neurons. To address this issue, we showed that the expression of mRNA for the markers of GABA-ergic neurons, i.e., GAD1 and glutamatergic neurons, i.e., VGlut2 did not change. Further, the expression of $Ca_V1.3_{42A}$ and $Ca_V1.3_{42}$ when normalized to GAD1 and VGltu2 expression did not differ in MPTP treated SNpc as compared to controls. (iii) The upregulation of $Ca_V1.3_{42A}$ and $Ca_V1.3_{42}$ mRNA results from their increased expression in the surviving TH neurons. In the light of the present results demonstrating a decrease in TH and DAT expression and an increase in $Ca_V1.3_{42A}$ and $Ca_V1.3_{42}$ mRNA levels, it is likely that the surviving DA neurons in SNpc are expressing greater levels of $Ca_V1.3_{42A}$ and $Ca_V1.3_{42}$ mRNA.

Further, an increase in the expression of $Ca_V1.3_{42A}$ upon normalization with TH and DAT 24 h after a single exposure to MPTP, in which case, there is no downregulation of TH and DAT also suggests that there is potentially an increase in the expression of $Ca_V1.3$ channels in vulnerable DA neurons in SNpc on exposure to MPTP.

This set of results supports the view that mouse DA neurons in SNpc may be more at risk to degenerate presumably because they have to cope with a larger influx of calcium through $Ca_V1.3$ L-type calcium channels during neurodegeneration (Surmeier and Schumacker, 2013). Possibly related to present observations, Lieberman et al. (2017) demonstrated that there is a build-up of cytosolic calcium in cultured DA neurons from SN as opposed to VTA following treatment with the active metabolite of MPTP, MPP^+. To conclude, the sustained high levels of expression of $Ca_V1.3_{42}$ and its variant $Ca_V1.3_{42A}$ indicates the possible contribution of these two channel isoforms to degeneration of dopaminergic neurons in the sub-chronic MPTP mouse model of PD.

DATA AVAILABILITY STATEMENT

The raw data supporting the conclusions of this article will be made available by the authors, without undue reservation, to any qualified researcher.

ETHICS STATEMENT

The animal study was reviewed and approved by Institutional Animal and Ethics Committee of Indian Institute of Science, Bangalore, India (Protocol# CAF/Ethics/267/2012).

AUTHOR CONTRIBUTIONS

The research project was conceptualized by VR, organized by AV and VR and executed by AV. Statistical analysis was designed and executed by AV and reviewed and critiqued upon by VR. First draft of the manuscript was written by AV and VR.

FUNDING

ACKNOWLEDGMENTS

SUPPLEMENTARY MATERIAL

The Supplementary Material for this article can be found online at: https://www.frontiersin.org/articles/10.3389/fnagi.2019.003 82/full#supplementary-material.

REFERENCES

Ayton, S., and Lei, P. (2014). Nigral iron elevation is an invariable feature of Parkinson's disease and is a sufficient cause of neurodegeneration. *Biomed. Res. Int.* 2014:581256. doi: 10.1155/2014/581256

Betarbet, R., Sherer, T. B., and Greenamyre, J. T. (2005). Ubiquitin-proteasome system and Parkinson's diseases. *Exp. Neurol.* 191, S17–S27. doi: 10.1016/j.expneurol.2004.08.021

Bock, G., Gebhart, M., Scharinger, A., Jangsangthong, W., Busquet, P., Poggiani, C., et al. (2011). Functional properties of a newly identified C-terminal splice variant of $Ca_V1.3$ L-type Ca^{2+} channels. *J. Biol. Chem.* 286, 42736–42748. doi: 10.1074/jbc.m111.269951

Brichta, L., and Greengard, P. (2014). Molecular determinants of selective dopaminergic vulnerability in Parkinson's disease: an update. *Front. Neuroanat.* 8:152. doi: 10.3389/fnana.2014.00152

Carvalho, A. N., Marques, C., Rodrigues, E., Henderson, C. J., Wolf, C. R., Pereira, P., et al. (2013). Ubiquitin-proteasome system impairment and MPTP-induced oxidative stress in the brain of C57BL/6 wild-type and GSTP knockout mice. *Mol. Neurobiol.* 47, 662–672. doi: 10.1007/s12035-012-8368-4

Chan, C. S., Gertler, T. S., and Surmeier, D. J. (2010). A molecular basis for the increased vulnerability of substantia nigra dopamine neurons in aging and Parkinson's disease. *Mov. Disord.* 25, S63–S70. doi: 10.1002/mds.22801

Chan, C. S., Guzman, J. N., Ilijic, E., Mercer, J. N., Rick, C., Tkatch, T., et al. (2007). 'Rejuvenation' protects neurons in mouse models of Parkinson's disease. *Nature* 447, 1081–1086. doi: 10.1038/nature05865

Chomczynski, P., and Sacchi, N. (2006). The single-step method of RNA isolation by acid guanidinium thiocyanate-phenol-chloroform extraction: twenty-something years on. *Nat. Protoc.* 1, 581–585. doi: 10.1038/nprot.2006.83

Damier, P., Hirsch, E. C., Agid, Y., and Graybiel, A. M. (1999). The substantia nigra of the human brain. I. Nigrosomes and the nigral matrix, a compartmental organization based on calbindin D_{28K} immunohistochemistry. *Brain* 122, 1421–1436. doi: 10.1093/brain/122.8.1421

Dauer, W., and Przedborski, S. (2003). Parkinson's disease: mechanisms and models. *Neuron* 39, 889–909. doi: 10.1016/s0896-6273(03)00568-3

Foehring, R. C., Zhang, X. F., Lee, J. C. F., and Callaway, J. C. (2009). Endogenous calcium buffering capacity of substantia nigral dopamine neurons. *J. Neurophysiol.* 102, 2326–2333. doi: 10.1152/jn.00038.2009

Gibb, W. R., and Lees, A. J. (1991). Anatomy, pigmentation, ventral and dorsal subpopulations of the substantia nigra and differential cell death in Parkinson's disease. *J. Neurol. Neurosurg. Psychiatry* 54, 388–396. doi: 10.1136/jnnp.54.5.388

Guzman, J. N., Ilijic, E., Yang, B., Sanchez-Padilla, J., Wokosin, D., Galtieri, D., et al. (2018). Systemic isradipine treatment diminishes calcium-

dependent mitochondrial oxidant stress. *J. Clin. Invest.* 128, 2266–2280. doi: 10.1172/jci95898

Guzman, J. N., Sanchez-Padilla, J., Wokosin, D., Kondapalli, J., Ilijic, E., Schumacker, P. T., et al. (2010). Oxidant stress evoked by pacemaking in dopaminergic neurons is attenuated by DJ-1. *Nature* 468, 696–700. doi: 10.1038/nature09536

Hirsch, E., Graybiel, A. M., and Agid, Y. A. (1988). Melanized dopaminergic neurons are differentially susceptible to degeneration in Parkinson's disease. *Nature* 334, 345–348. doi: 10.1038/334345a0

Huang, H., Yu, D., and Soong, T. W. (2013). C-terminal alternative splicing of Ca$_V$1.3 channels distinctively modulates their dihydropyridine sensitivity. *Mol. Pharmacol.* 84, 643–653. doi: 10.1124/mol.113.087155

Ilijic, E., Guzman, J. N., and Surmeier, D. J. (2011). The L-type channel antagonist isradipine is neuroprotective in a mouse model of Parkinson's disease. *Neurobiol. Dis.* 43, 364–371. doi: 10.1016/j.nbd.2011.04.007

Jackson-Lewis, V., and Przedborski, S. (2007). Protocol for the MPTP mouse model of Parkinson's disease. *Nat. Protoc.* 2, 141–151. doi: 10.1038/nprot. 2006.342

Kang, Y., and Kitai, S. T. (1993). Calcium spike underlying rhythmic firing in dopaminergic neurons of the rat substantia nigra. *Neurosci. Res.* 18, 195–207. doi: 10.1016/0168-0102(93)90055-u

Khaliq, Z. M., and Bean, B. P. (2010). Pacemaking in dopaminergic ventral tegmental area neurons: depolarizing drive from background and voltage-dependent sodium conductances. *J. Neurosci.* 30, 7401–7413. doi: 10.1523/JNEUROSCI.0143-10.2010

Lieberman, O. J., Choi, S. J., Kanter, E., Saverchenko, A., Frier, M. D., Fiore, G. M., et al. (2017). α-synuclein-dependent calcium entry underlies differential sensitivity of cultured SN and VTA dopaminergic neurons to a Parkinsonian neurotoxin. *eNeuro* 4:ENEURO.0167–17.2017. doi: 10.1523/ENEURO.0167-17.2017

Liss, B., and Striessnig, J. (2019). The potential of L-type calcium channels as a drug target for neuroprotective therapy in Parkinson's disease. *Annu. Rev. Pharmacol. Toxicol.* 59, 263–289. doi: 10.1146/annurev-pharmtox-010818-021214

Mercuri, N. B., Bonci, A., Calabresi, P., Stratta, F., Stefani, A., and Bernardi, G. (1994). Effects of dihydropyridine calcium antagonists on rat midbrain dopaminergic neurones. *Br. J. Pharmacol.* 113, 831–838. doi: 10.1111/j.1476-5381.1994.tb17068.x

Michel, P. P., and Hefti, F. (1990). Toxicity of 6-hydroxydopamine and dopamine for dopaminergic neurons in culture. *J. Neurosci. Res.* 26, 428–435. doi: 10.1002/jnr.490260405

Michel, P. P., Hirsch, E. C., and Hunot, S. (2016). Understanding dopaminergic cell death pathways in Parkinson disease. *Neuron* 90, 675–691. doi: 10.1016/j. neuron.2016.03.038

Nair-Roberts, R. G., Chatelain-Badie, S. D., Benson, E., White-Cooper, H., Bolam, J. P., and Ungless, M. A. (2008). Stereological estimates of dopaminergic, GABAergic and glutamatergic neurons in the ventral tegmental area, substantia nigra and retrorubral field in the rat. *Neuroscience* 152, 1024–1031. doi: 10.1016/j.neuroscience.2008.01.046

Nedergaard, S., and Greenfield, S. A. (1992). Sub-populations of pars compacta neurons in the substantia nigra: the significance of qualitatively and quantitatively distinct conductances. *Neuroscience* 48, 423–437. doi: 10.1016/0306-4522(92)90502-s

Park, J., Kim, Y., and Chung, J. (2009). Mitochondrial dysfunction and Parkinson's disease genes: insights from *Drosophila. Dis. Model. Mech.* 2, 336–340. doi: 10.1242/dmm.003178

Pifl, C., Rajput, A., Reither, H., Blesa, J., Cavada, C., Obeso, J. A., et al. (2014). Is Parkinson's disease a vesicular dopamine storage disorder? Evidence from a study in isolated synaptic vesicles of human and nonhuman primate striatum. *J. Neurosci.* 34, 8210–8218. doi: 10.1523/JNEUROSCI.5456-13.2014

Saeed, U., Karunakaran, S., Meka, D. P., Koumar, R. C., Ramakrishnan, S., Joshi, S. D., et al. (2009). Redox activated MAP kinase death signaling cascade initiated by ASK1 is not activated in female mice following MPTP: novel mechanism of neuroprotection. *Neurotox. Res.* 16, 116–126. doi: 10.1007/s12640-009-9058-5

Schapira, A. H. V. (2013). Calcium dysregulation in Parkinson's disease. *Brain* 136, 2015–2016. doi: 10.1093/brain/awt180

Schapira, A. H. V., Cooper, J. M., Dexter, D., Clark, J. B., Jenner, P., and Marsden, C. D. (1990). Mitochondrial complex I deficiency in Parkinson's disease. *J. Neurochem.* 54, 823–827. doi: 10.1111/j.1471-4159.1990.tb02325.x

Sherman, M. Y., and Goldberg, A. L. (2001). Cellular defenses against unfolded proteins: a cell biologist thinks about neurodegenerative diseases. *Neuron* 29, 15–32. doi: 10.1016/s0896-6273(01)00177-5

Singh, A., Gebhart, M., Fritsch, R., Sinnegger-Brauns, M. J., Poggiani, C., Hoda, J.-C., et al. (2008). Modulation of voltage- and Ca^{2+}-dependent gating of Ca$_V$1.3 L-type calcium channels by alternative splicing of a C-terminal regulatory domain. *J. Biol. Chem.* 283, 20733–20744. doi: 10.1074/jbc.m802 254200

Sofic, E., Riederer, P., Heinsen, H., Beckmann, H., Reynolds, G. P., Hebenstreit, G., et al. (1988). Increased iron (III) and total iron content in post mortem substantia nigra of parkinsonian brain. *J. Neural Transm.* 74, 199–205. doi: 10.1007/bf01244786

Surmeier, D. J., and Schumacker, P. T. (2013). Calcium, bioenergetics, and neuronal vulnerability in Parkinson's disease. *J. Biol. Chem.* 288, 10736–10741. doi: 10.1074/jbc.r112.410530

Surmeier, D. J., Guzman, J. N., and Sanchez-Padilla, J. (2010). Calcium, cellular aging and selective neuronal vulnerability in Parkinson's disease. *Cell Calcium* 47, 175–182. doi: 10.1016/j.ceca.2009.12.003

Surmeier, D. J., Guzman, J. N., Sanchez-Padilla, J., and Schumacker, P. T. (2011). The role of calcium and mitochondrial oxidant stress in the loss of substantia nigra pars compacta dopaminergic neurons in Parkinson's disease. *Neuroscience* 198, 221–231. doi: 10.1016/j.neuroscience.2011.08.045

Surmeier, D. J., Schumacker, P. T., Guzman, J. D., Ilijic, E., Yang, B., and Zampese, E. (2017). Calcium and Parkinson's disease. *Biochem. Biophys. Res. Commun.* 483, 1013–1019. doi: 10.1016/j.bbrc.2016.08.168

Tan, B. Z., Jiang, F., Tan, M. Y., Yu, D., Huang, H., Shen, Y., et al. (2011). Functional characterization of alternative splicing in the C terminus of L-type Ca$_V$1.3 channels. *J. Biol. Chem.* 286, 42725–42735. doi: 10.1074/jbc.M111. 265207